Electrical Bistability and Memory Phenomenon in Carbon Nanotube-Conjugated Polymer Matrixes

Basudev Pradhan, Sudip K. Batabyal, and Amlan J. Pal*

Department of Solid State Physics, Indian Association for the Cultivation of Science, Kolkata 700 032, India

Received: January 7, 2006; In Final Form: March 1, 2006

We have observed electrical bistability and large conductance switching in functionalized carbon nanotube (CNT)-conjugated polymer composites at room temperature. The concentration of the CNTs in the polymer matrix controlled the degree of bistability. Conduction mechanism applicable in each of the conducting states has been identified. The switching had an associated memory phenomenon and was reversible in nature. In the bistable devices, the active layer retained its high-conducting state until a reverse voltage erased it. We could "write" or "erase" a state and "read" it for many cycles for random-access memory applications.

1. Introduction

Carbon nanotubes are unique nanostructures with remarkable electronics and mechanical properties.[1] It has opened up newer possibilities for novel components in miniaturized electronic devices.[2] Initial interests on carbon nanotubes (CNTs) were due to their exotic electronic structures. As other fascinating properties were discovered, such as amazing electronic transport properties, unique Raman spectra, and unusual mechanical strength, interests grew and led to their potential use in nanometer-sized electronics and a variety of other applications.[2−12] To date, various types of molecular devices such as field-effect transistors (FET),[3−7] logic gate circuits, inverters, optoelectronic, and transistor memory devices[8−12] have been fabricated.

Because of a high mobility of CNTs, stored charges led to memory applications in FET structures.[9−12] Transport processes and work-function of the CNTs, in conjunction with suitable molecular orbitals of conjugated polymers, may provide interesting characteristics as devices; electrical bistability with associated memory phenomenon can be one such application of interest. In electrical bistable devices,[13,14] two conductivities or current levels are observed at one voltage. The switching between the states can be associated with a memory phenomenon (memory switching[13]) and can lead to read-only and random-access memory elements.

CNTs' applications in molecular scale devices are somewhat restricted due to their insolubility in common solvents and hence difficulties in homogeneous film formation. In general, dispersion of CNTs is obtained with the aid of a high-power ultrasonic probe.[15,16] To achieve homogeneous films of soluble CNTs and facilitate charge conduction, we targeted to use functionalized CNTs.[17−20] The chemical modification of CNTs is an emerging area in materials science. Among the various approaches, the most general one is esterification of oxidized nanotubes.[19] CNTs in such homogeneous films in polymer matrix would act as carrier trapping centers and control transport though the matrix. In this Article, we show how the conductance of the system can be switched to yield bistable devices with memory phenomenon.

* Corresponding author. Telephone: +91-33-24734971 (ext. 313). Fax: +91-33-24732805. E-mail: sspajp@iacs.res.in.

2. Experimental Section

Multiwalled CNTs were purchased from Aldrich Chemical Co. The outer diameter, wall thickness, length, and purity were 20−30 nm, 1−2 nm, 0.5−2.0 mm, and >95%, respectively. The regioregularity of poly(3-hexyl thiophene) (P3HT), also purchased from Aldrich, was 98%. The CNTs were functionalized following the route proposed by Qin et al.[17] They were first converted to its acid form via sonication in a concentrated nitric acid−sulfuric acid mixture (1:3) at 50 °C for 6 h. Excess acids were removed by centrifuging in deionized water repeatedly till the pH of water became around 7. The acid form of CNT was converted to sodium salt, which was refluxed with tetra-*n*-butylammonium bromide and butyl bromide for 8 h so that esterified CNTs precipitate out of the solution. The unfunctionalized part was removed by dissolving the esterified part in chloroform. With the addition of ethanol, the functionalized CNT precipitated out and was dried in a vacuum at 50 °C. The functionalization process was monitored by FT-IR studies after every reaction step. The spectrum of the final product showed the presence of C═O and C−H stretching vibrations due to the ester groups.

Devices were fabricated on indium tin oxide (ITO)-coated glass substrates, which were cleaned and processed following standard protocol. P3HT was first dissolved in chloroform (1.2 mg/mL). A measured amount of esterified CNT was added to P3HT solution to obtain a homogeneous mixture. The amount of CNT was 0.04 and 0.4 mg per 1 mL of P3HT solution. Pure P3HT solution and P3HT−CNT solutions were spun on ITO-coated glass substrates at a speed of 1000 rpm for 30 s. The thin films, which had a thickness of 50−70 nm, were annealed at 60 °C in a vacuum (10^{-3} Torr) for 2 h. Aluminum (Al) was vacuum-evaporated on top of the annealed films from a tungsten filament basket at a pressure below 10^{-5} Torr. The active areas of each of the devices, ITO/P3HT/Al (device 1), ITO/P3HT:CNT (3.3%)/Al (device 2), and ITO/P3HT:CNT (33%)/Al (device 3), were 6 mm^2.

The devices were characterized in a shielded vacuum chamber with a Yokogawa 7651 dc source and a Keithley 486 picoammeter. Bias was applied with respect to the Al electrode and up to a different maximum voltage (V_{Max}) and changed in steps of 0.05 V. Device current was measured after 20 s, resulting in a sweep rate of 2.5 mV/s. The dc source, coupled with fast

10.1021/jp060122z CCC: $33.50
Published on Web 04/01/2006

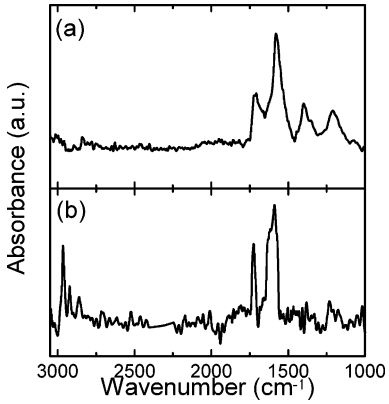

Figure 1. FT-IR spectra of (a) carboxylate CNTs and (b) esterified CNTs. The latter figure shows additional C−H and C−O stretching vibrations.

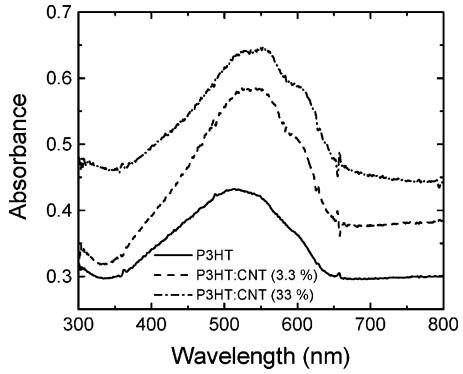

Figure 2. Absorbance spectra of P3HT, P3HT:CNT (3.3%), and P3HT:CNT (33%) thin films on quartz substrates.

switching transistors, was used to generate voltage pulses of different widths and amplitudes, which were used to "write", or "read", or "erase" a state of the devices. Impedance spectroscopy of the devices was carried out with a Solartron 1260 Impedance Analyzer in the 1 Hz to 12 MHz frequency range. A 100 mV rms signal was used as a test voltage. Measurements were carried out without any dc bias and in a parallel mode configuration. The instruments were controlled with a personal computer via a general-purpose interface bus (GPIB). UV−vis absorption spectra of the films, deposited on quartz substrates, were recorded with a Hewlett-Packard UV−vis spectrophotometer HP-8453. Field emission scanning electron microscope (FE-SEM) images ware taken with a JEOL JSM-6700F.

3. Results and Discussion

The functionalization process of the CNTs was monitored through FT-IR spectra of the intermediate products. The FT-IR spectra of the CNTs with carboxylic acid groups and butyl substitution are shown in Figure 1a and b, respectively. The presence of C═C stretching vibrations of the CNT backbones is observed at 1580 cm^{-1} in both of the materials. The peaks at 1209 and 1716 cm^{-1} refer to C−O and C═O stretching vibrations of the carboxylic acid group, respectively.[18,20] In butyl-substituted nanotubes, additional C−H stretching vibrations of the alkyl chain appeared at 2965, 2923, and 2859 cm^{-1}. The C−O stretching vibration of ester appeared at 1726 cm^{-1}.[18]

The UV−vis absorbance spectra of the different composite films are shown in Figure 2. P3HT films show absorption bands at 440 and 550 nm. Addition of CNTs in P3HT provided a featureless absorption profile with a gradual increase toward

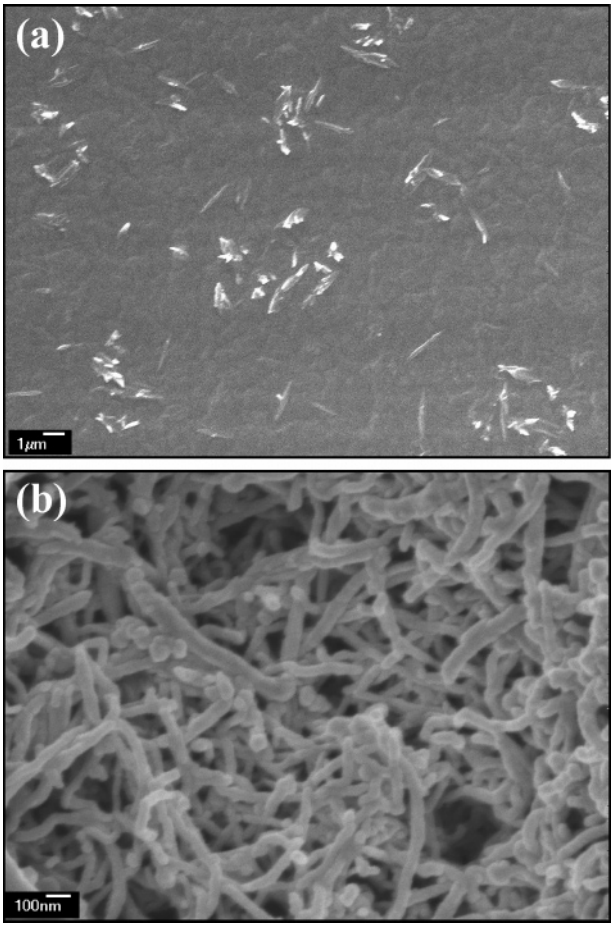

Figure 3. SEM image of (a) P3HT:CNT (33%) thin films and (b) CNTs surrounded by the polymers. The increase in diameter in the latter image as compared to the former one is due to polymer-coating of the nanotubes.

the UV region. Because of the presence of CNTs in the polymer matrix, there was no shift in the absorption bands, suggesting that there was no interaction between the polymer and the CNTs in their ground states.

Because of the functional groups of the CNTs, the nanotubes could be homogeneously dispersed in the polymer matrix. The field emission scanning electron microscope (FE-SEM) image of a P3HT:CNT film (33%) on an ITO substrate, as displaced in Figure 3a, shows the level of homogeneity. To check the degree of adhesion of the nanotubes and the polymers, a little amount of P3HT solution was added to the functionalized CNT powders. The FE-SEM picture of a drop-cast film, which contained largely CNTs, is shown in Figure 3b. The picture shows that the diameter of the tubes with the polymer was around 40−50 nm. The diameter was much higher in contrast to that of the pristine tubes, which was around 20 nm. This shows that the polymer chains embedded the nanotubes closely.

$I-V$ characteristics of the devices were recorded by scanning applied voltage from 0 to $+V_{Max}$ and then to $-V_{Max}$ followed by a reverse scan from $-V_{Max}$ to $+V_{Max}$. We have varied the amplitude of V_{Max} to generate a range of $I-V$ characteristics. The characteristics were nonlinear in nature during repeated voltage cycles. Typical characteristics in devices with CNT showed electrical bistability (Figure 4). Device current at any voltage during the sweep from $-V_{Max}$ was several orders higher in magnitude as compared to that during the sweep from $+V_{Max}$. The increase in conductivity at $-V_{Max}$, or conductance switching, was associated with a memory phenomenon. In other words, no bias was required to sustain the higher conducting state,

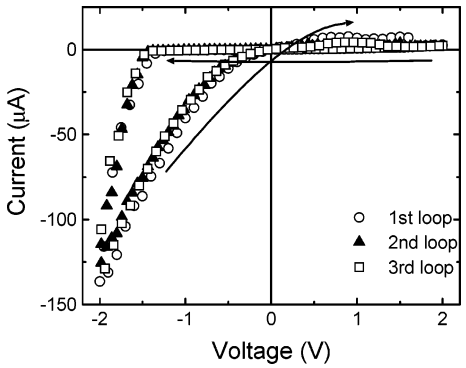

Figure 4. $I-V$ characteristics of a device based on spin-cast films of P3HT:CNT (33%) in three consecutive voltage loops. Arrows show the sweep direction of the applied voltage.

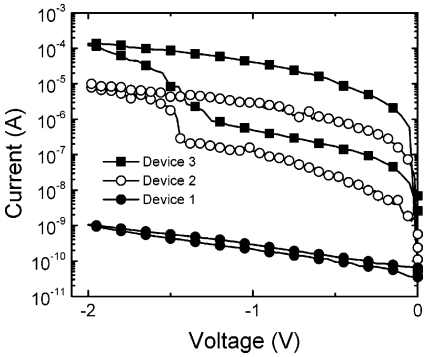

Figure 5. Reverse bias section of $I-V$ characteristics of devices based on P3HT (device 1), P3HT:CNT (3.3%) (device 2), and P3HT:CNT (33%) (device 3) in the two sweep directions. Amplitude of device current has been plotted.

which was induced by a negative bias. Only a suitable positive bias could switch the high-conducting state to a low one. The figure further shows that the current values retraced during the voltage cycles. Hence, the transitions between the two states were reproducible.

To study the role of CNTs in the polymer matrix on electrical bistability of the devices, we have compared $I-V$ characteristics of the three devices (Figure 5). In the voltage range of our measurement, the devices with pristine P3HT did not show any change in conductivity during the two sweep directions. Both of the devices with CNTs exhibited reproducible bistability and transition to a high-conducting state. The devices started to switch from a low-conducting state at around -1.4 V. With increase in CNT concentration in the polymer matrix, current for both of the conducting states increased. The ratio between the currents in the two-states, the on/off ratio, also increased with CNT concentration. The ratio, which depended also on the voltage at which it was measured, was 24 and 60 at -2 V in device 2 and device 3, respectively.

FET structures based on CNTs in inert polymer matrixes as active channels exhibited memory phenomenon.[9−12] During gate voltage sweep, reconfiguration of charge carriers occurred in the system leading to memory effect. Electrical bistability was observed also in a somewhat similar sandwich structure with gold nanoparticles or C_{60} embedded in an inert polymer environment as active layer.[21−23] The switching was proposed to be due to electric-field-induced charge transfer between the nanoparticle and their conjugated capping. In the present case with CNTs in conjugated environment, electron transfer may occur at a suitable bias from the CNTs to the lowest unoccupied molecular orbital (LUMO) of the polymer, leading to an increase in conductivity of the system. In fact, the difference between

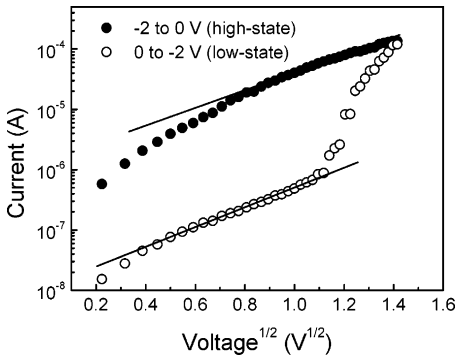

Figure 6. Current versus square root of voltage amplitude of a device based on P3HT:CNT (33%) film low- and high-conducting states. Results from the reverse bias section of $I-V$ characteristics are plotted here. The lines are best fit to the linear regime of the plot in each case.

the Fermi level of CNTs (5.1 eV) and LUMO of P3HT (3.53 eV) is 1.57 eV, which is close to the voltage (1.44 V) at which transition to the high-conducting state occurred (Figures 4 and 5).

From the $I-V$ characteristics in the high- and low-conducting states, conduction mechanism has been studied. The nonlinear $I-V$ in the two states can be plotted as $\log(I)$ versus $V^{1/2}$ (Figure 6). For the two conducting states, that is, for voltage sweeps from 0 to $-$ 2 V and from -2 to 0 V representing low- and high-conducting states, respectively, the plots fit to straight lines, suggesting that the conduction mechanism followed thermionic emission model.[24] According to this model, current density (J) at a field (F) is given by:

$$J = AT^2 \exp[-(\phi - \beta F^{1/2})/kT]$$

where A is a constant, T is the temperature, ϕ is the energy barrier with the electrode, and β relates the relative dielectric constant (ϵ_r) of the material as $\beta = (e^3/4\pi\epsilon_0\epsilon_r)^{1/2}$. Here, ϵ_0 is permittivity of free space and e is the electronic charge. For the two conducting-states, the slope of the plot did not change, especially in the high-field region, suggesting that the dielectric constant remained unaltered during the transition. The intercept with the abscissa, however, differed in the two states. For the high-conducting state, the extrapolated intercept at 0 V was more and hence the barrier with the electrode was less as compared to that in the low-conducting state. The decrease in ϕ should be due to a decrease in energy barrier height at the metal/film interface upon electron transfer from the CNTs. In the low-field region, we observed a deviation from the linear behavior. The mechanism involved in the low-field region is not totally clear. It could be due to a change in some field-dependent components, for example, width of tunneling barrier, in the conduction mechanism process.

To further rule out a role of conformational change or variation of dielectric properties during conductance switching, we have measured impedance characteristics of the devices. Cole−Cole plots exhibited a perfect semicircle, suggesting that the devices can be modeled as a parallel combination of a resistor and a capacitor. After each of the states was induced by a suitable voltage, frequency dependence of dielectric constant was recorded at 0 V. Figure 7 shows such a plot for the two states. The figure shows that the dielectric constant changed marginally in the two conducting states. The thermionic emission plot (Figure 6) also exhibited little or no change in dielectric constant. The results therefore show that the change in resistive properties, as dictated by the band gap of the material and correspondingly barrier height with the metal electrodes at the interfaces, controls electrical bistability in these devices.

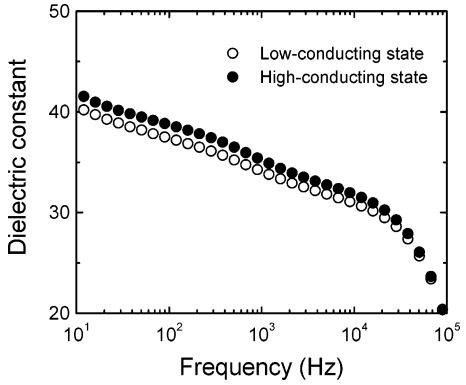

Figure 7. Frequency response of real part of dielectric function at zero dc bias for the two states of a device based on P3HT:CNT (33%) films.

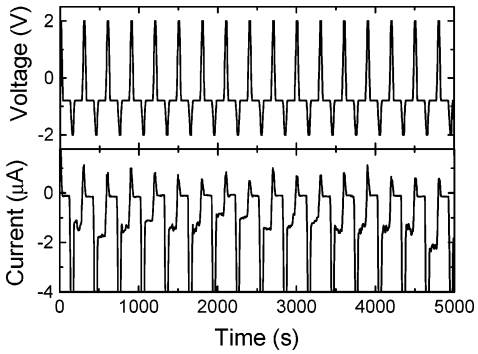

Figure 8. Switching performance of a device based on P3HT:CNT (33%) during a continuous "write−read−erase−read" sequence. The voltage pulse is shown in the upper trace, while the current response is shown in the lower one. The high-conducting state has been induced ("write") by the −2 V pulse, while the low-one has been reinstated ("erase") by +2 V. Between switching, the states were probed ("read") by measuring current under a small voltage (−0.8 V).

Reversibility of the associated memory phenomenon can best be studied under a voltage pulse sequence, "write−read−erase−read" cycle. In such a cycle, the high- and low-conducting states are induced ("write" and "erase", respectively) repeatedly and the states are monitors or "read" in between. We have characterized the devices under such voltage sequence for up to 30 h. A section of the voltage sequence and corresponding current from a device with 33% of CNT is shown in Figure 8. Here, −2 and +2 V pulses (width = 15 s) were applied to "write" the high-state and "erase" to a low-conducting one, respectively. The states were probed by a measuring device current at −0.8 V. The figure shows that the magnitude of current under "read" voltage was much higher during probing the high-conducting state as compared to the low-state. The results hence show that one can flip-flop the two states of the devices and probe them successfully as in rewritable or random-access memory (RAM) applications.

4. Conclusion

In conclusion, we have functionalized CNTs with butyl groups so that homogeneous films can be formed with P3HT as a matrix material. We have observed electrical bistability in P3HT:CNT films. The transition to a high-conducting state has been explained in terms of charge transfer from the CNTs to conjugated polymer chains. The ratio between the conductances of the high- and low-states increased with an increase in CNT concentration in the polymer matrix. The transitions between the two states were rewritable in nature and associated with memory phenomenon. The devices exhibited random-access memory applications under "write−read−erase−read" voltage sequence. The conduction mechanisms in the two conducting states have been modeled by considering a change in band gap and correspondingly a decrease in barrier height with the electrodes.

Acknowledgment. We acknowledge valuable discussion with S. Manna of the Polymer Science Unit regarding the FTIR analysis. We also acknowledge financial support from the Department of Science and Technology, Government of India, through project SP/S2/M-44/99.

References and Notes

(1) Iijima, S. *Nature* **1991**, *354*, 56−58.
(2) Baughman, R. H.; Zakhidov, A. A.; de Heer, W. A. *Science* **2002**, *297*, 787−792.
(3) Tans, S. J.; Verschueren, A. R. M.; Dakker, C. *Nature* **1991**, *393*, 49−52.
(4) Fuhrer, M. S.; Kim, B. M.; Brintlinger, T. *Nano Lett.* **2002**, *2*, 755−759.
(5) Klinke, C.; Chen, J.; Afzali, A.; Avouris, P. *Nano Lett.* **2005**, *5*, 555−558.
(6) Snow, E. S.; Campbell, P. M.; Ancona, M. G.; Novak, J. P. *Appl. Phys. Lett*. **2005**, *86*, 033105.
(7) Fan, R.; Yue, M.; Karnik, R.; Majumdar, A.; Yang, P. *Phys. Rev. Lett.* **2005**, *95*, 086607.
(8) Star, A.; Lu, Y.; Bradley, K.; Gruner, G. *Nano Lett.* **2004**, *4*, 1587−1591.
(9) Cui, J. B.; Sordan, R.; Burghard, M.; Kern, K. *Appl. Phys. Lett.* **2002**, *81*, 3260−3262.
(10) Ganguly, U.; Kan, E. C.; Zhang, Y. *Appl. Phys. Lett.* **2005**, *87*, 043108.
(11) Wang, S.; Sellin, P. *Appl. Phys. Lett.* **2005**, *87*, 133117.
(12) Naber, R. C. G.; Boer, B. D.; Blom, P. W. M.; Leeum, D. M. *Appl. Phys. Lett.* **2005**, *87*, 203509.
(13) Bandhopadhyay, A.; Pal, A. J. *J. Phys. Chem. B* **2003**, *107*, 2531−2536.
(14) Chu, C. W.; Ouyang, J.; Tseng, J.-H.; Yang, Y. *Adv. Mater*. **2005**, *17*, 1440−1443.
(15) Kymakis, E.; Amaratunga, G. A. J. *Appl. Phys. Lett.* **2002**, *80*, 112−114.
(16) Bhattacharyya, S.; Kymakis, E.; Amaratunga, G. A. J. *Chem. Mater*. **2004**, *16*, 4819−4823.
(17) Chen, J.; Hamon, M. A.; Hu, H.; Chen, Y.; Rao, A. M.; Eklund, P. C.; Haddon, R. C. *Science* **1998**, *282*, 95−98.
(18) Qin, Y.; Shi, J.; Wu, W.; Li, X.; Guo, Z. X.; Zhu, D. *J. Phys. Chem. B* **2003**, *47*, 12899−12908.
(19) Hirsch, A. *Angew. Chem., Int. Ed.* **2002**, *41*, 1853−1862.
(20) Liu, L.; Qin, Y.; Guo, Z.-X.; Zhu, D. *Carbon* **2003**, *41*, 331−335.
(21) Ouyang, J.; Chu, C.-W.; Szmanda, C. R.; Ma, L.; Yang, Y. *Nat. Mater.* **2004**, *3*, 918−922.
(22) Ouyang, J.; Chu, C.-W.; Sieves, D.; Yang, Y. *Appl. Phys. Lett.* **2005**, *86*, 123507.
(23) Paul, S.; Kanwal, A.; Chhowalla, M. *Nanotechnology* **2006**, *17*, 145−151.
(24) Kao, K. C.; Hwang, W. In *Electrical Transport in Solids, International Series in the Science of Solid State*; Pamplin, B. R., Ed.; Pergamon Press: Oxford, 1981; Vol. 14, pp 64−144.